Cellulose (2021) 28:259–271
https://doi.org/10.1007/s10570-020-03530-x

ORIGINAL RESEARCH

Effects of hemicellulose composition and content on the interaction between cellulose nanofibers

Akio Kumagai · Takashi Endo

Received: 27 March 2020 / Accepted: 14 October 2020 / Published online: 26 October 2020

Abstract In this study, cellulose nanofibers (CNFs) from softwood and hardwood kraft pulps were prepared with different hemicellulose contents, and the effects of the hemicellulose compositions and contents on the interaction between CNFs were studied. In addition, the effects of CNF interaction on the CNF dispersion stability and viscosity characteristics in the aqueous state were investigated. Using quartz crystal microbalance with dissipation, the results of the interaction analysis revealed that hemicellulose moderated the strength of the interaction between CNFs, and the intensity of the interaction changed according to the hemicellulose compositions. The interaction between galactoglucomannans was stronger than that between glucuronoxylans, and CNFs prepared from softwood pulp containing mainly galactoglucomannan showed stronger interaction between CNFs than those prepared from hardwood pulp containing mainly glucuronoxylan. The presence of hemicelluloses on the surface of CNFs improved the dispersion stability and increased the viscosity. However, the intensity of the interaction between CNFs, which is dependent on the type of hemicellulose, did not affect these properties. The properties of CNFs in the aqueous state are determined by not only the interaction between CNFs but also several factors such as the morphology of CNFs and physical properties of hemicelluloses.

Keywords Cellulose nanofiber · Hemicellulose · Softwood · Hardwood · Dispersion stability · Viscosity

Introduction

Cellulose nanofibers (CNFs) have recently received attention as nanomaterials prepared from wood sources and non-wood sources, including agricultural residue and industrial waste (Siró and Plackett 2010; Pennells et al. 2020). CNFs are prepared from these plant raw materials by mechanical fibrillation such as grinding, homogenization, and ultrasonication (Pääkkö et al. 2007; Klemm et al. 2011). By combining chemical treatments such as 2,2,6,6-tetramethylpiperidine-1-oxyl (TEMPO)-oxidation, phosphorylation, and esterification of maleic anhydride, more uniform and fine CNFs can be prepared (Isogai et al. 2011; Noguchi et al. 2017; Iwamoto and Endo 2015). The main components of

Electronic supplementary material The online version of this article (https://doi.org/10.1007/s10570-020-03530-x) contains supplementary material, which is available to authorized users.

A. Kumagai (✉) · T. Endo
Research Institute for Sustainable Chemistry, Department of Materials and Chemistry, National Institute of Advanced Industrial Science and Technology (AIST), 3-11-32 Kagamiyama, Higashi-Hiroshima, Hiroshima 737-0046, Japan
e-mail: a-kumagai@aist.go.jp

plant cell walls are cellulose, hemicellulose, and lignin, and the chemical composition of these components do not change significantly when CNFs are produced only by mechanical fibrillation. Thus, the saccharide compositions of CNFs reflect the composition of the raw materials (Solala et al. 2020). Cellulose is a linear homopolysaccharide composed of glucose, and several types of hemicelluloses are heteropolysaccharides composed of hexoses (e.g., mannose, glucose, galactose), pentoses (e.g., xylose, arabinose), and sugar acids (e.g. glucuronic acid) (Scheller and Ulvskov 2010). Xylans are the main hemicellulose found in angiosperms such as hardwoods (dicotyledons or dicots) and herbaceous plants (monocotyledons or monocots), while glucomannans and xylans are the main hemicelluloses in gymnosperms such as softwoods. Xylans are composed of a β-(1 → 4)-linked xylopyranosyl backbone, and several types are present depending on the substituents. Xylans in hardwoods (dicots) are glucuronoxylans, of which the substituents are α-(1 → 2)-linked 4-*O*-methyl-glucopyranosyl uronic acid and acetyl groups; the main substituents of herbaceous plants (monocots) are (1 → 3)- and/or (1 → 2)-linked arabinofuranosyl units. Xylans in softwoods are arabinoglucuronoxylans, of which the substituents are α-(1 → 3)-linked arabinofuranosyl and α-(1 → 2)-linked 4-*O*-methyl-glucopyranosyl uronic acid. Galactoglucomannans in softwoods comprise a backbone with β-(1 → 4)-linked mannopyranosyl and glucopyranosyl units, with backbone substitutions of α-(1 → 6)-linked galactopyranosyl and acetyl groups. Thus, there are differences between hemicelluloses that constitute softwoods and hardwoods. Furthermore, these hemicelluloses are present on cellulose microfibrils, and the laminated structure of hemicelluloses differ between softwoods and hardwoods (Kumagai and Endo 2018).

Generally, CNFs prepared from lignin-removed kraft pulps are often used in CNF research. The CNFs prepared from softwood and hardwood pulps have different properties, e.g. the viscosities of TEMPO-oxidized CNFs differ between softwood and hardwood pulps (Mendoza et al. 2018). The films prepared from CNFs produced by mechanical fibrillation indicate a significant difference in the breaking strain between softwood and hardwood pulps (Stelte and Sanadi 2009). The CNF raw materials prepared by mechanical fibrillation after either enzymatic hydrolysis or TEMPO-oxidation also significantly affect the structural, morphological, optical, mechanical, thermal, and hydrophobic properties of CNF films (Yadong et al. 2017). These different properties depending on the types of pulps used as CNF raw materials are influenced by the morphology and crystallinity of CNFs (Stelte and Sanadi 2009; Yadong et al. 2017; Mendoza et al. 2018). The morphology is affected by pulp tree species and excessive treatment (Stelte and Sanadi 2009), and the crystallinity is affected by amorphous region of CNFs (Yadong et al. 2017; Mendoza et al. 2018).

It is known that hemicellulose contributes to efficient fibrillation and dispersion stability of CNFs by electric and/or steric mechanisms other than crystallinity. The efficient fibrillation is due to pulp swelling caused by hemicelluloses, which have higher accessibility to water than cellulose (Tenhunen et al. 2014; Kulasinski et al. 2015). The presence of hemicellulose prevents coalescence of CNFs, which also contributes to efficient fibrillation (Iwamoto et al. 2008). Hemicelluloses like xylans have a carboxyl group which provide a net negative charge, and side chains which contribute to the steric repulsion; these structural features influence the dispersion stability of CNFs (Tenhunen et al. 2014). In addition, structurally different hemicelluloses interact differently with CNFs prepared from softwood and hardwood pulps. Galactoglucomannans in softwood, for instance, have a higher affinity for CNFs prepared from softwood pulp than for those prepared from hardwood pulp due to the difference composition of hemicelluloses on the CNF surface (Eronen et al. 2011).

This study aimed to understand how CNFs with different hemicellulose compositions interact and affect the properties of CNFs in the aqueous state. CNFs with different hemicellulose compositions and contents were prepared by hemicellulase treatment using softwood and hardwood pulps as raw materials. The interaction between CNFs was examined using quartz crystal microbalance with dissipation (QCM-D), which was also used to analyze the interaction of hemicellulose with CNFs, and the surface constitutions of hemicelluloses on CNFs (Eronen et al. 2011; Kumagai and Endo 2018). We also studied how the hemicellulose composition-dependent interaction between CNFs, influenced the dispersion stability and the viscosity characteristics of CNF dispersions.

Materials and methods

Materials

Never-dried bleached pine and eucalyptus kraft pulps were used as the starting material to prepare CNFs with different hemicellulose compositions from softwood and hardwood, respectively. These kraft pulps were purchased from Marusumi Paper Co. Ltd. (Ehime, Japan). The pulps, cut into small pieces, were immersed in deionized water (5 wt%) and stirred until they were sufficiently swollen slowly. The swollen pulps were then fibrillated using a disk mill (Supermasscolloider MKCA6-2, Masuko Sangyo Co. Ltd., Saitama, Japan) equipped with two nonporous ceramic disks. First, pre-refining was performed by treating multiple passes ($\sim$50) with wide clearance between the two disks (1000–300 μm). Fibrillation of the pulps was then performed with ten passes, while gradually decreasing the clearance between the two disks to 150 μm. These fibrillations using a disk mill were performed at a rotation speed of 1800 rpm. After adjusting the disk-milled pulp content to 1 wt% with ultrapure water and dispersing by ultrasonication using an ultrasonic generator (US-150T, Nissei Co. Ltd., Tokyo, Japan), further fibrillation was performed with ten passes through a high-pressure homogenizer (Masscomizer MMX-L100, Masuko Sangyo Co. Ltd., Saitama, Japan) at a pressure of approximately 200 MPa. Pure CNF without hemicellulose was also prepared from cotton cellulose powder (Whatman CF11, GE Healthcare, Illinois, USA) using the same procedure except for the pre-refining step. CNFs with decreasing hemicellulose content were prepared by enzymatic hydrolysis with commercial purified enzymes before high-pressure treatment. The enzymatic hydrolysis was performed in 50 mM sodium acetate buffer (pH 5.0) at 40 °C for 48 h using *Aspergillus niger* endo-1,4 β-mannanase and endo-1,4-β-xylanase (Megazyme Int. Ireland Ltd., County Wicklow, Ireland). After terminating the enzymatic reaction by soaking in a hot water bath (105 °C, 10 min), the enzyme-treated disk-milled pulps were washed thoroughly with ultrapure water before high-pressure treatment. The homogenized CNFs (1 wt%) prepared from pulps were gel-like and viscous. The prepared CNFs were stored at 4 °C until further use. Commercial low-viscosity glucomannan (60% mannose, 40% glucose) from konjac and glucuronoxylan (82.3% xylose, 12.8% glucuronic acid, and 4.9% other sugars) from beechwood were used as pure hemicelluloses (Megazyme Int. Ireland Ltd., County Wicklow, Ireland).

Characterization of CNFs

After sulfuric acid hydrolysis to monosaccharides, based on the laboratory analytical procedures of the National Renewable Energy Laboratory with some modifications, was performed according to our previous study (Kumagai et al. 2013), the carbohydrate compositions of the CNFs were determined using high-performance liquid chromatography.

The total charge (anionic charge) of prepared CNFs was analyzed by conductometric titration according to the standard titration method (SCAN CM 65:02) using an automated titrator (AUT-701, DKK-TOA Co., Tokyo, Japan).

The morphologies of CNFs were observed using a field-emission scanning electron microscope (FE-SEM) (S-4800, Hitachi High-Technologies Co., Tokyo, Japan) at 1 kV. The CNFs were freeze-dried to preserve their original structure after washing with *tert*-butyl alcohol several times until all the water had been replaced. The prepared samples were coated with an approximately 0.5 nm-thick layer of osmium using an osmium coater (Neoc-ST, Meiwafosis, Co., Tokyo, Japan).

The surface topologies of CNFs were characterized by atomic force microscopy (AFM) (JSPM-5200, JEOL Co. Ltd., Tokyo, Japan). The CNF dispersions, which were diluted to 0.001–0.005 wt% and ultrasonicated for 1 min to prevent aggregation and improve their dispersibility, were dried on a silicon wafer. AFM characterization of CNFs on a silicon wafer was performed in tapping mode using aluminum reflex-coated silicon cantilevers (PPP-NCHR, Nano World AG, Neuchâtel, Switzerland) in the presence of air at 25 °C.

Interaction analysis by QCM-D

The interaction between CNFs was studied using a QCM-D apparatus (Q-Sense E1, Biolin Scientific AB, Götenborg, Sweden) (Rodahl et al. 1995; Reviakine et al. 2011). QCM-D is extremely sensitive in measuring the adsorption of material onto a quartz crystal from the shift in the resonant frequency of the

quartz crystal. The change in absorbed mass per unit surface (Δm) is estimated from the shift in the resonant frequency (Δf) using the Sauerbrey equation (Sauerbrey 1959; Höök et al. 1998) (1),

$$\Delta m = -\frac{C\Delta f}{n} \quad (1)$$

where C is the sensitivity constant (0.177 mg/m^2) and n is the overtone number. The Sauerbrey equation is accurately suited only in the case of rigid and uniform thin layers, and the approximation underestimates the adsorbed mass in the case of viscoelastic materials.

The QCM-D apparatus evaluates the viscoelastic properties of the adsorbed viscoelastic materials (Rodahl et al. 1995; Höök et al. 1998; Reviakine et al. 2011). The viscoelastic material adsorbed on the sensor surface causes frictional loss that damps the oscillation with a decay rate of amplitude depending on the viscoelastic properties of the material. This is measured as the dissipation factor (D) defined as Eq. (2),

$$D = \frac{E_{\text{diss}}}{2\pi E_{\text{stored}}} \quad (2)$$

where E_{diss} is the dissipated energy during one oscillation cycle, and E_{stored} is the total energy stored in the oscillation. The viscoelastic materials with faster decreasing oscillation indicate more extensive changes in the dissipation factors.

Prepared CNFs were coated on QCM-D gold sensor (QSX 301, Biolin Scientific AB, Götenborg, Sweden) according to previous studies (Ahola et al. 2008 and Kumagai et al. 2013). The supernatants of 0.1 wt% CNF dispersions were prepared using centrifugation for 30 min at 10,000 rpm after they were diluted to 0.1 wt% and ultrasonicated for 1 min. The supernatants were placed on the QCM-D gold sensor, pre-absorbed with 1 wt% polyethyleneimine (Mw 70,000), incubated for 1 min, and then spin-coated at 3000 rpm for 1 min. The CNF spin-coated sensors were rinsed with ultrapure water, dried gently with nitrogen gas, and heated at 80 °C for 10 min in an oven. The sensor surfaces were analyzed using AFM to confirm whether CNF coating was suitable for QCM-D analysis (Figure S1). In addition, the areal masses of CNF-coated sensors were calculated from the frequency changes before and after coating based on Eq. (1), and it was confirmed that each CNF indicated a comparable areal mass. The in situ adsorption of each CNF on CNF-coated sensors was monitored with a QCM-D apparatus, and the interactions were evaluated as the change in oscillating frequency and dissipation factor. The CNF-coated sensor was assembled in the QCM-D flow chamber; ultrapure water was pumped through the sensor chamber until the frequency and dissipation signals stabilized, indicating that the CNF on CNF-coated sensor was sufficiently swollen and stabilized. After the profiles of frequency and dissipation reached a plateau, each 0.1 wt% CNF suspension was introduced and allowed to adsorb for 20 min. Then, ultrapure water was introduced to wash out unadsorbed CNFs for more than 10 min. Additionally, 0.01 wt% hemicellulose (glucomannan and glucuronoxylan) was used to analyze the interaction between the hemicelluloses and CNF films. All QCM-D analyses were performed with a controlled flow rate of 50 µL/min at 25 °C. Changes in the frequency were recorded at the fundamental resonance frequency (5 MHz), and its third overtone (15 MHz) was used for data profiling.

Evaluation of dispersion stability using stability analyzer

The stability of CNF dispersions was evaluated using a stability analyzer (Turbiscan Tower, Formulaction Inc., Toulouse, France). CNF dispersions at 0.05 wt% were measured in a cylindrical glass cell (sample volume of 20 mL, sample height of 40 mm), where the optical reading head was scanned from the bottom to the top by a near-infrared light source (λ = 850 nm), with scanning time from 0 to 24 h at intervals of 30 min at 25 °C. The concentration of CNF dispersions was chosen as previously published (Tenhunen et al. 2014), the dispersion stability of the CNF dispersion diluted to 0.05 wt% was evaluated after the dispersion was sufficiently achieved by ultrasonication for 1 min. The results were analyzed using the Turbiscan Stability Index (TSI), which provided information on the general behavior of dispersions to compare and characterize the physical stability. TSI was calculated as the sum of all the scan differences in the destabilization processes performed with the Turbiscan software.

Viscosity measurement by rheometer

Rheological testing was performed using a rheometer (ARES G2, TA Instruments, Delaware, USA) with a cone-and-plate geometry (cone angle, 1° 59′ 20″; diameter, 40 mm) to investigate the viscosity characteristics of CNF dispersions. The shear flow properties of 0.5 wt% CNF dispersions were measured at a shear rate ranging from 0.1 to 100 s^{-1} at 25 °C under a solvent-trap cover.

Results and discussion

Characteristics of prepared CNFs

A series of CNFs were prepared from softwood and hardwood pulp raw materials with different hemicellulose contents to investigate the effect of hemicellulose composition on the interaction between CNFs prepared from kraft pulps. Table 1 shows the saccharide compositions of the prepared CNFs in this study. In general, the major hemicelluloses in softwood are galactoglucomannan and arabinoglucuronoxylan, and in hardwood, it is glucuronoxylan (Scheller and Ulvskov 2010). The results of the saccharide composition showed that the softwood and hardwood pulps used as the raw materials for CNFs contained general hemicelluloses (Table 1). Each pulp was treated with mannase and xylanase for 48 h to remove these hemicelluloses, while none of the hemicelluloses was completely hydrolyzed. According to a previous study, loosely bound fractions of xylan can be hydrolyzed with xylanase, but xylan fractions that are more tightly associated with cellulose cannot be removed with xylanase (Penttilä et al. 2013). In this study, CNFs with high (H) and low (L) hemicellulose contents were prepared from softwood (SW-CNF) and hardwood (HW-CNF) pulps with and without hemicellulase treatment, respectively (Table 1). In addition, CNF prepared from cotton cellulose powder (CP-CNF) containing no hemicellulose was also obtained for comparison.

The charge provided by hemicellulose is one of the critical factors in considering the interaction between CNFs. The total charges determined by the conductometric titration are shown in Table 1, along with the conductivity and the pH of CNF dispersions. All CNF dispersions had comparable conductivity and pH, but the values of total charge differed in correlation with the hemicellulose content. SW-CNF(H) and HW-CNF(H) with high hemicellulose contents had higher values of total charge, and pure CP-CNF containing no hemicellulose had the lowest values of total charge. Both softwood and hardwood pulps contain xylans with glucuronic acid, which have a negative charge in the side chain (Scheller and Ulvskov 2010). Thus, it is suggested that xylans contribute to the total charge value. HW-CNFs containing more xylans had slightly higher absolute total charge values than SW-CNFs (Table 1).

Figure 1 shows microscopic images of CNFs prepared from each wood pulp. Although the hemicellulose compositions and contents of all CNFs are different (Table 1), their morphologies were very similar (Fig. 1). Therefore, it is difficult to judge the difference in the characteristics of these CNFs from the observed images of both FE-SEM and AFM. The similar morphologies of CNFs prepared from softwood and hardwood pulps (Eronen et al. 2011), and the morphologies of CNFs that are not significantly changed by the removal of hemicelluloses using

Table 1 Saccharide composition, total charge, conductivity and pH of CNFs

Sample	Saccharide composition (%)					Total charge (μmol/g)	Conductivity (mS/m)	pH
	Glucose	Xylose	Mannose	Galactose	Arabinose			
CP-CNF	100.9	n.d.	n.d.	n.d.	n.d.	14	0.215	6.2
SW-CNF(H)	84.7	7.7	6.0	0.5	0.8	39	0.307	6.1
SW-CNF(L)	93.6	2.8	1.8	0.2	0.3	25	0.282	6.3
HW-CNF(H)	75.1	21.6	n.d.	n.d.	n.d.	52	0.357	6.1
HW-CNF(L)	90.1	7.6	n.d.	n.d.	n.d.	21	0.254	6.3

CP cellulose powder; *SW* softwood; *HW* hardwood; *H* high hemicellulose content; *L* low hemicellulose content; *n.d.* not detected

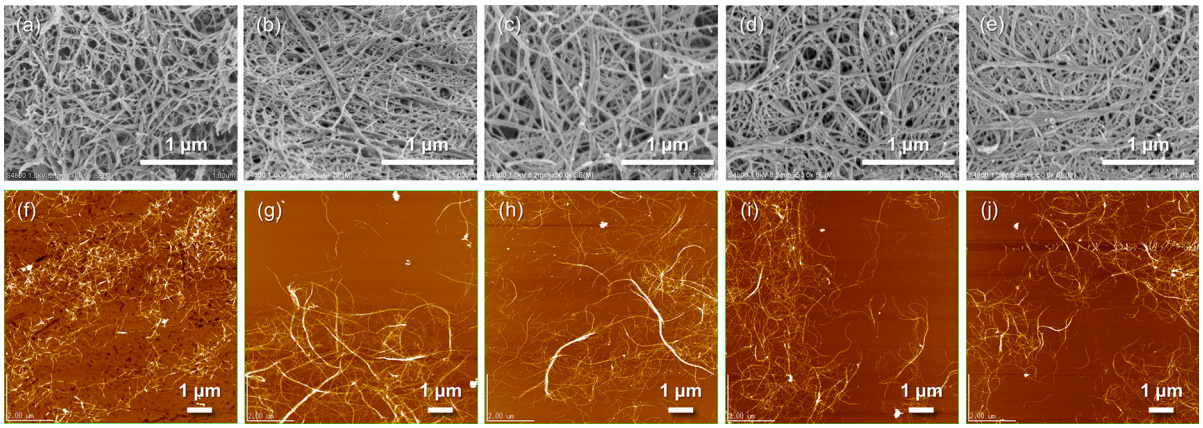

Fig. 1 Field-emission scanning electron microscopy (FE-SEM) images (**a**–**e**) and atomic force microscopy (AFM) height images (**f**–**j**) of CNFs prepared from cotton cellulose powder (CP), softwood (SW), and hardwood (HW) pulps with adjusted hemicellulose contents. **a**, **f** CP-CNF, **b**, **g** SW-CNF-High hemicellulose (H), **c**, **h** SW-CNF-Low hemicellulose (L), **d**, **i** HW-CNF(H), **e**, **j** HW-CNF(L)

enzymatic hydrolysis correspond with previous studies (Arola et al. 2013). Although it is difficult to determine the fiber length by microscopic observation, the observation results show that fiber diameters were very similar for all CNFs (Fig. 1). The fiber length of CNFs depends on the raw material, the pretreatment, and the fibrillation process (Stelte and Sanadi 2009; Mendoza et al. 2018). In general, the fiber length of SW-CNFs was longer than those of HW-CNFs. Thus, the CNF morphologies were similar, and the localization of the hemicelluloses could not be confirmed by microscopic observation. However, the laminated structures of the hemicelluloses are located around the cellulose microfibrils of CNFs in different layers depending on the raw material (Kumagai and Endo 2018). Therefore, the interaction between CNFs is likely to be affected by the compositions and contents of hemicelluloses.

Interaction between CNFs

The interaction between CNFs in the aqueous state was investigated using QCM-D to determine the effect of the compositions and contents of hemicelluloses on the surface properties of CNFs. QCM-D is a useful technique for in situ adsorption studies at the solid/liquid interface such as antigen–antibody interactions and enzymatic reactions (Höök et al. 1998; Kumagai et al. 2013). Figure 2a shows the frequency changes monitored using QCM-D, indicating the adsorption and desorption behavior occurring on the quartz crystal sensor. The decrease in frequency indicated that the introduced CNFs were adsorbed on the CNF-coated quartz crystal sensor. The strength of the relative interaction between CNFs could be evaluated by comparing the frequency changes.

Pure CP-CNF prepared from cotton powder without hemicelluloses showed much larger frequency change than CNFs prepared from other wood pulps, as shown in Fig. 2a. In CNFs prepared from softwood and hardwood pulps, SW-CNF(H) and HW-CNF(H), which have high hemicellulose contents, showed small changes in frequency, while SW-CNF(L) and HW-CNF(L) with reduced hemicellulose contents by enzymatic treatment showed larger frequency changes. The QCM-D results suggest that hemicelluloses on the surface of CNFs inhibit the strong interaction between cellulose microfibrils in the aqueous state.

Figure 2b shows the dissipation changes, monitoring of which enables further interpretation of the viscoelasticity of the adsorbed layer on the quartz crystal sensor (Voinova et al. 1999). As shown in Eq. (2), the dissipation factor is defined as the ratio of dissipated energy to stored energy when oscillating stress is applied to the sensor surface layer, and the change in dissipation represents the structural change that occurs under stress. As shown in Fig. 2, the amount of change in dissipation corresponded to the amount of change in frequency, and the order of magnitude of both changes coincided with each other. That is, pure CP-CNF showed the largest change in

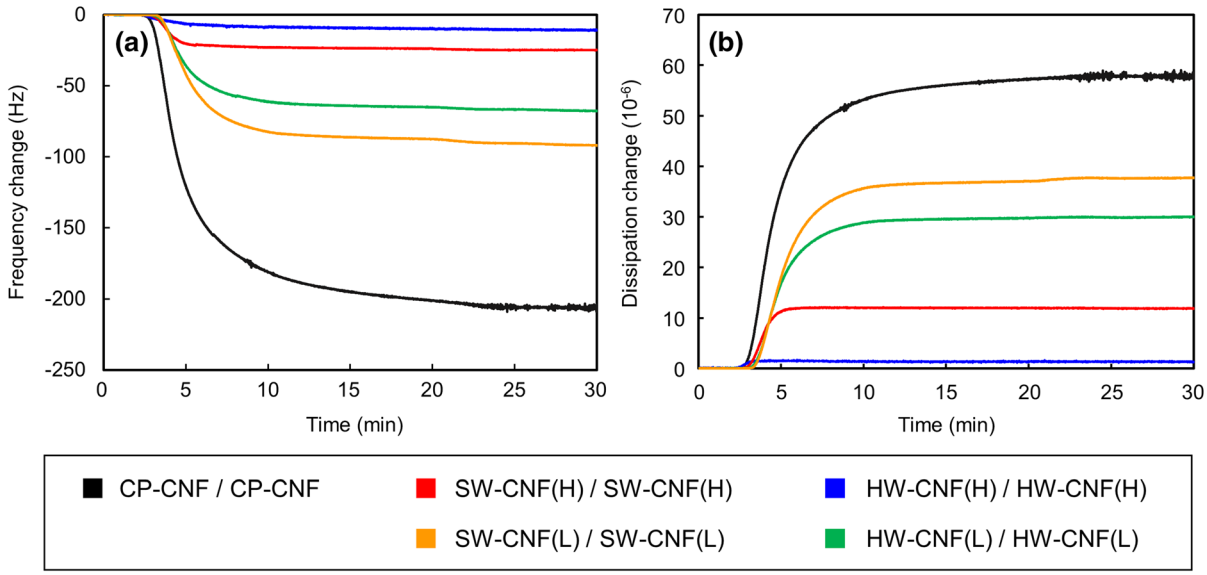

Fig. 2 Changes in the frequency (**a**) and dissipation (**b**) of CNFs on the same CNF films analyzed using quartz crystal microbalance with dissipation (QCM-D). Changes in the frequency were measured at the third overtone of the 5 MHz fundamental frequency. The left is CNF films coated on the sensor, and the right is the CNFs introduced for adsorption, separated by a slash in the explanatory notes. CP: cotton cellulose powder; HW: hardwood; SW: softwood; H: high hemicellulose; L: low hemicellulose

dissipation, followed by SW-CNF(L) and HW-CNF(L) with low hemicellulose content, and SW-CNF(H) and HW-CNF(H) with high hemicellulose content showed the smallest change in dissipation. This result implies that the viscoelasticity of the adsorbed CNF layer depends on the type and content of hemicellulose.

To evaluate the viscoelastic properties of the adsorbed CNFs on the sensor, we plotted the change in dissipation (ΔD) as the function of the change in frequency (Δf) (Fig. 3). The viscoelastic property is correlated with the slope of the resulting curve (ΔD–Δf profile). The lower the slope, the more rigid is the adsorbed layer, whereas if the slope becomes steeper, it indicated that the layer is becoming softer and more mobile (Tammelin et al. 2006). Regarding the slopes of ΔD–Δf profiles at the initial adsorption stage (Fig. 3b), the slopes between CNFs with equivalent hemicellulose content were comparable. The higher the hemicellulose content, the steeper the initial ΔD–Δf profiles; the most gentle initial ΔD–Δf profile was that of CP-CNF without hemicellulose (Fig. 3b). The shape of ΔD–Δf profiles (Fig. 3) due to the slight changes in frequency and dissipation (Fig. 2) shown by SW-CNF(H) and HW-CNF(H) with high hemicellulose content are typical of polyelectrolyte-type adsorption rather than that of relatively large macromolecules such as CNF. It seems that the repulsion caused by hemicellulose prevented the significant adsorption between the cellulose microfibrils. On the other hand, CP-CNF and the CNFs with lower hemicellulose content showed linear ΔD–Δf profiles (Fig. 3). The perfectly linear relationship of ΔD–Δf profiles indicates the formation of a dense and compact adsorption layer (Tammelin et al. 2006), suggesting that these CNFs are strongly adsorbed. These results prove that the amount of hemicellulose in CNFs affects the adsorption of CNFs, as well as and the viscoelastic properties of the CNF adsorption layer.

SW-CNF and HW-CNF which have different hemicellulose compositions showed different frequency changes compared with each other, and SW-CNF showed a larger increase in frequency than HW-CNF in both CNFs with high and low hemicellulose contents (Fig. 2). The different interactions between SW-CNF and HW-CNF were probably attributed to the difference in the interaction strength between the hemicelluloses. Therefore, the interaction of major hemicelluloses contained in each pulp with SW-CNF

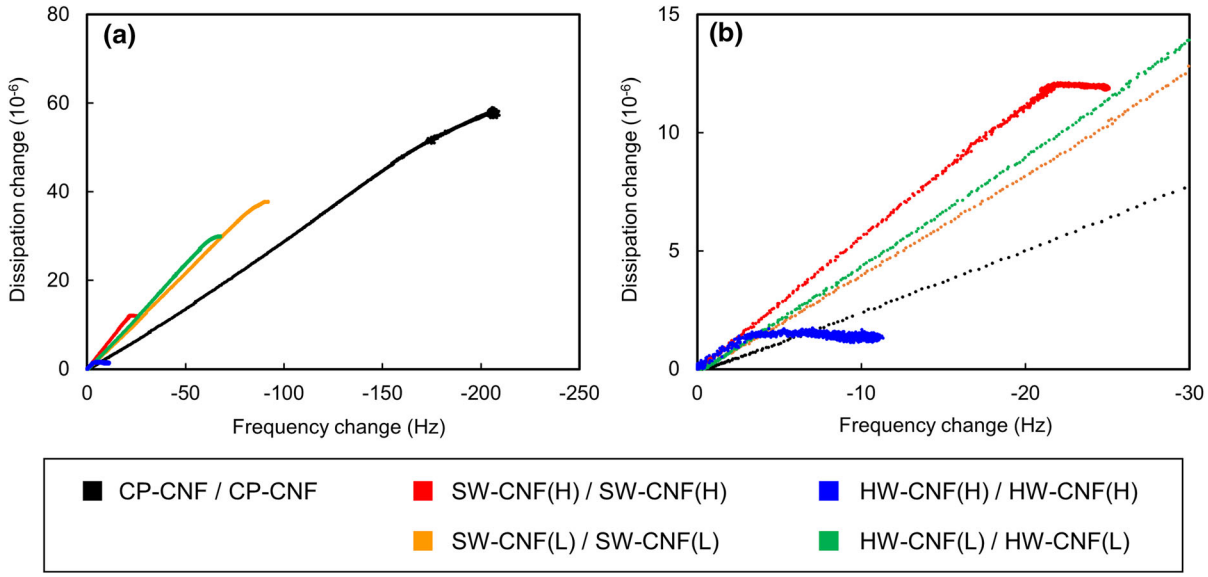

Fig. 3 The relationship between the change in dissipation (ΔD) and the change in frequency (Δf) during 30 min of CNF adsorption on the same CNF film: **a** full range; **b** restricted range (ΔD: 0–15; Δf: − 30–0). Changes in the frequency were measured at the third overtone of the 5 MHz fundamental frequency. The left is CNF films coated on the sensor, and the right is the CNFs introduced for adsorption, separated by a slash in the explanatory notes. CP: cotton cellulose powder; HW: hardwood; SW: softwood; H: high hemicellulose; L: low hemicellulose

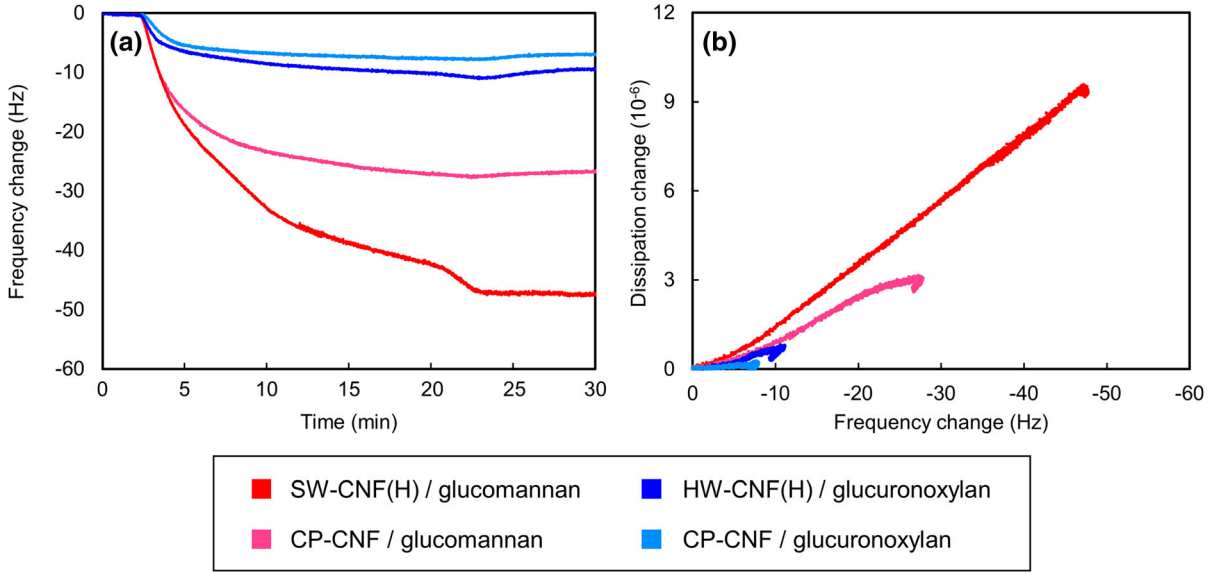

Fig. 4 Adsorption of hemicelluloses on the CNF films: **a** frequency change over time; **b** relation between the change in dissipation (ΔD) and the change in frequency (Δf) during 30 min of hemicellulose adsorption on the CNF films. Changes in the frequency were measured at the third overtone of the 5 MHz fundamental frequency. The left is CNF films coated on the sensor and the right is the hemicelluloses introduced for adsorption, separated by a slash in the explanatory notes. CP: cotton cellulose powder; HW: hardwood; SW: softwood; H: high hemicellulose

and HW-CNF was analyzed using QCM-D (Fig. 4). As mentioned in the saccharide composition (Table 1), softwood is rich in galactoglucomannan, and the major hemicellulose of hardwood is glucuronoxylan. The changes in frequency shown in Fig. 4a indicate that the adsorption of glucomannan on SW-CNF is larger than that of glucuronoxylan on HW-CNF. This association of galactoglucomannan to CNF prepared from softwood pulp corresponds with previous studies investigating the interactions of structurally different native hemicelluloses with CNF prepared from several wood pulps using QCM-D (Eronen et al. 2011). Similarly, the QCM-D results investigating the adsorption of hemicelluloses on pure CP-CNF showed that the interaction of cellulose with glucomannan was more potent than with glucuronoxylan (Fig. 4a). The high affinity of glucomannan for cellulose has also been suggested in a study conducting a dynamic mechanical analysis of softwood and bacterial cellulose cultivation in the presence of hemicelluloses (Salmén and Olsson 1998; Tokoh et al. 2002). Further, the slope of ΔD–Δf profile correlated with the amount of hemicellulose adsorption (Fig. 4b). That is, glucomannan, which showed a larger frequency change, showed a linear ΔD–Δf profile with a steeper slope. Meanwhile, the low increase in dissipation ($\Delta D < 1 \times 10^{-6}$) of glucuronoxylan indicates its adsorbed layer is rigid. Hemicellulose is adsorbed irreversibly on both cellulose and other hemicelluloses (Tammelin et al. 2009), and the adsorption properties of hemicellulose on cellulose is influenced by the structure of the hemicellulose (Eronen et al. 2011). Thus, it is suggested that the interactions between CNFs prepared from wood pulps are affected by the properties of the hemicelluloses on the surface of CNFs.

Dispersion stability of CNFs

The dispersion stabilities of CNFs were investigated to evaluate whether the interaction between CNFs, which changed with the compositions and contents of hemicelluloses as revealed by QCM-D, affects the properties of CNF in an aqueous state. Precisely 0.05 wt% dilute CNF dispersions that can avoid CNF networks which are formed at high concentration, were evaluated using a stability analyzer, Turbiscan, to accurately evaluate the influence of hemicellulose (Tenhunen et al. 2014). This analyzer enables the evaluation of migration-related phenomena such as creaming and sedimentation, and the changes in particle size such as coalescence and flocculation, by monitoring transmittance and backscattering in the vertical axis direction (Tenhunen et al. 2014; Olejnik et al. 2015). Figure 5 shows the transmittance profile of the CNF dispersions every 2 h recorded for 24 h. The horizontal axis represents the height of the cylindrical glass cell containing CNF dispersion, while the vertical axis indicates the transmittance. Based on various conditions, such as concentration, fiber length and diameter, and chemical composition, CNFs dispersed in water aggregate and settle out, and the shape of the transmittance profile changes significantly (Kumagai et al. 2019). However, as shown in Fig. 5, none of the CNFs showed any changes in the shape of the transmittance profile, indicating sedimentation. At the same time, it was reported that CNF derived from birch kraft pulp with reduced xylan content show a transmittance profile indicating gradual sedimentation in 20 min in the evaluation of dispersion stability at the same concentration (0.05 wt%) of dilute CNF dispersions (Tenhunen et al. 2014). Although the transmittance profile showing the dispersion of SW-CNF(H), which had high dispersion stability, showed almost no change even after 24 h (Fig. 5a), the transmittances of SW-CNF(L) and HW-CNF(L) dispersions with low hemicellulose contents changed over time without the profile change (Fig. 5b, d). These dispersions of CNFs with low hemicellulose contents formed fine floating aggregates. However, the fine aggregates did not settle out due to Brownian motion because dilute CNF dispersions were used to avoid CNF network formation in this study. Although it is difficult to compare them because of the different designs of experiments, the total charge of CNFs from pine and eucalyptus kraft pulps (25 and 21 μmol/g) with reduced hemicellulose content prepared in this study was higher than that of CNFs from birch kraft pulp (13 μmol/g) as described by Tenhunen et al. (2014). Therefore, CNFs from pine and eucalyptus pulps in this study did not show Turbiscan profile changes, indicating the apparent sedimentation, like the CNFs from the birch pulp reported in a previous study (Tenhunen et al. 2014). The relationship between the total charge and the results of Turbiscan suggests that the surface charge provided by hemicellulose is involved in the dispersion stability of CNFs.

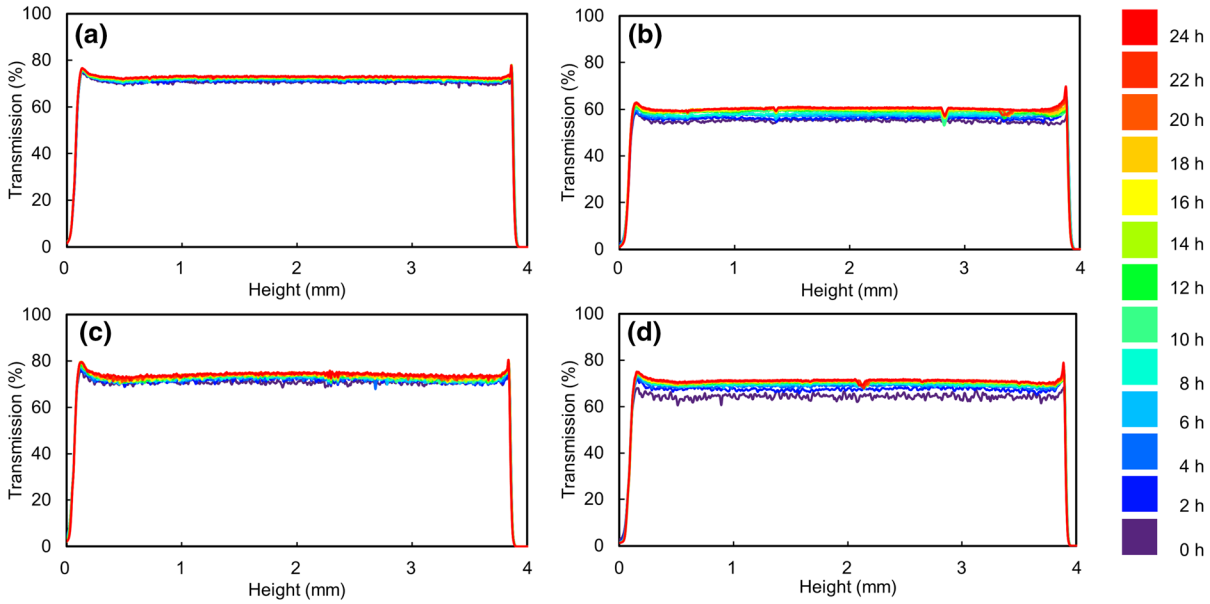

Fig. 5 Light transmittance profiles of the CNF dispersions evaluated using stability analyzer every 2 h recorded for 24 h. **a** SW-CNF(H), **b** SW-CNF(L), **c** HW-CNF(H), **d** HW-CNF(L). HW: hardwood; SW: softwood; H: high hemicellulose; L: low hemicellulose

It is difficult to compare the transmittance profile differences between the samples because the changes in the dispersion stability profiles obtained in this study are small (Fig. 5). Therefore, TSI, which is the index for comparing different dispersion stabilities calculated as the sum of all the scan differences of the transmittance profiles, was used for comparison (Fig. 6). The more stable dispersion indicates the lower value of the TSI (Olejnik et al. 2015). The TSI of the HW-CNF(L) dispersion greatly fluctuated compared with the other CNF dispersions immediately after the start of the measurement. This result indicated that the HW-CNF(L) dispersion aggregated earlier than the other CNF dispersions. In contrast, the result of the TSI of SW-CNF(H), which showed a small and gradual change, indicated that the SW-CNF(H) dispersion had high stability. Comparing the hemicellulose contents, the changes in TSI of SW-CNF(H) and HW-CNF(H) were smaller than those of SW-CNF(L) and HW-CNF(L). These results showed that CNF dispersions with lower hemicellulose contents had lower dispersion stability and tended to aggregate easily. Thus, hemicelluloses on the surface of CNFs, which cause steric hindrance and electrostatic repulsion, contributed to the improvement of dispersion stability in addition to the reduction of interactions between CNFs.

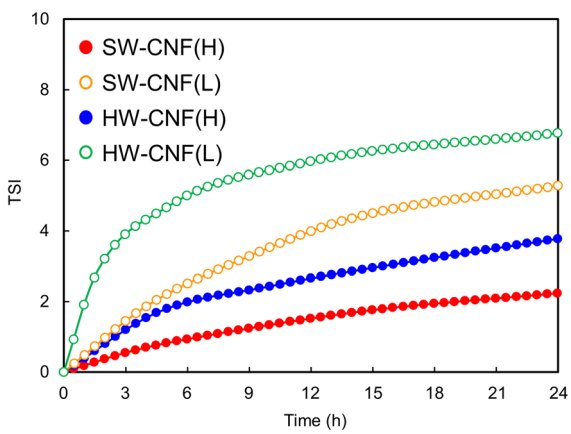

Fig. 6 Turbiscan Stability Index (TSI) over 24 h of CNFs prepared from softwood and hardwood pulps with adjusted hemicellulose contents. HW: hardwood; SW: softwood; H: high hemicellulose; L: low hemicellulose

Conversely, when SW-CNFs and HW-CNFs were compared, the changes in the TSI of SW-CNFs were smaller than of HW-CNFs. These results showed that SW-CNFs had higher dispersion stability than HW-CNFs. However, the interaction analysis using QCM-D suggested that SW-CNFs had stronger interaction with CNFs than HW-CNFs (Fig. 2). Additionally, the total charge, which is an important parameter indicating the dispersion stability, was also lower in SW-

CNFs than in HW-CNFs (Table 1). Based on these properties related to hemicelluloses on the surface of CNFs, lower dispersion stability of SW-CNFs than HW-CNFs was estimated. It was also reported that CNFs with longer fiber length tend to exhibit higher dispersion stability due to the CNF network formation, and SW-CNFs prepared by only mechanical fibrillation have a longer fiber length than HW-CNFs prepared by the same method (Stelte and Sanadi 2009). Besides, the mass change differences in QCM-D and the total charge between SW-CNFs and HW-CNFs were smaller than those between high and low hemicellulose contents. Therefore, multiple factors were involved in the dispersion stability of CNFs, and the influence of the fiber length of CNFs on the dispersion stability was greater than the electrostatic repulsion and the interaction between CNFs caused by hemicelluloses. Furthermore, although hemicelluloses on the surface of CNFs affected the improvement in dispersion stability of CNFs, the hemicellulose compositions probably had a relatively small effect on the dispersion stability of CNFs.

Viscosity characteristics of CNFs

In addition to investigating the dispersion stabilities of CNFs, the shear flow properties were investigated to evaluate whether the interaction between CNFs, which changed with the compositions and contents of hemicellulose revealed by QCM-D, affected the viscosity characteristics of CNFs. The viscosity profiles as a function of shear rate of each CNF dispersion prepared from different pulp sources are presented in Fig. 7. All the CNF dispersions exhibited shear-thinning properties, in which the viscosity decreased with increased shear rate. This viscosity characteristic is generally found in CNF dispersions (Nechyporchuk et al. 2016). The viscosity of CNF dispersion depends on the fiber length and diameter of CNF. Increasing the number of mechanical fibrillation leads to a smaller fiber diameter of CNF, and the viscosity of the CNF dispersion gradually increases (Lasseuguette et al. 2008; Grüneberger et al. 2014). The fiber length of CNF is determined by the raw material and the ease of fibrillation, and longer CNFs show higher viscosity (Iwamoto et al. 2014; Li et al. 2015; Mendoza et al. 2018). When we compared CNFs prepared from different types of wood pulp, SW-CNFs with a longer fiber length showed higher viscosity than HW-CNFs. Since interaction analysis using QCM-D showed that SW-CNFs had a more robust interaction than HW-CNFs, the interaction between CNFs also probably contributed to the higher viscosity of the dispersion of SW-CNFs (Fig. 2).

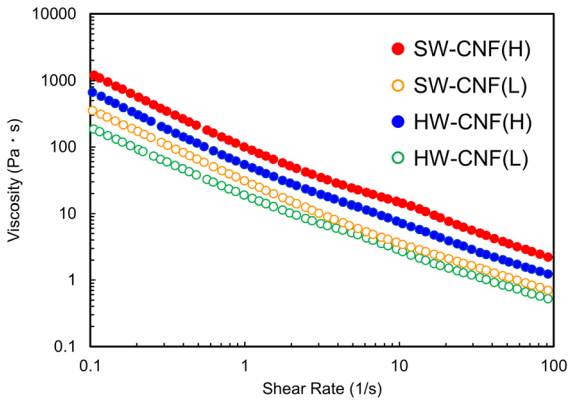

Fig. 7 Viscosity profiles as a function of shear rate of CNFs prepared from softwood and hardwood pulps with adjusted hemicellulose contents. HW: hardwood; SW: softwood; H: high hemicellulose; L: low hemicellulose

Focusing on the relationship between hemicellulose contents and viscosity characteristics, interaction analysis using QCM-D showed that SW-CNF(L) and HW-CNF(L) with lower hemicellulose content had stronger interactions among CNFs (Fig. 2), but SW-CNF(L) and HW-CNF(L) with lower hemicellulose content showed a lower viscosity than SW-CNF(H) and HW-CNF(H) with a higher hemicellulose content (Fig. 7). It is difficult to interpret the mechanism by which hemicellulose removal affects the viscosity characteristics of CNF dispersions. A previous study reported that the enzymatic hydrolysis of xylan leads to an apparent increase in the elastic modulus of the CNFs prepared from hardwood pulp without mixing. However, the enzymatic hydrolysis of xylan with continuous mixing lowers the elastic modulus of the CNFs (Arola et al. 2013). Enhancing the interaction between CNFs by removing hemicellulose made the CNF network stronger and increased the viscosity of the CNF dispersion. However, the removal of hemicellulose simultaneously lowered the dispersion stability, so that the aggregation of CNFs was induced by mixing, and the viscosity of the CNF dispersion was reduced. Although further investigation is needed to elucidate the mechanism of the effect of hemicelluloses on viscosity, this study also indicated that hemicelluloses had a considerable effect on

the viscoelastic characteristics of CNF dispersions. However, the strength of the interaction between CNFs depending on the hemicellulose compositions had no significant effect on the viscoelastic characteristics of CNF dispersions.

Conclusions

General CNFs prepared from kraft pulps have different hemicellulose compositions depending on the types of pulps. In this study, the interaction between CNFs prepared from kraft pulp with different hemicellulose compositions and contents were investigated, and the effect of the interaction on physical properties, such as dispersion stability and viscosity, and characteristics in the aqueous state were studied. Interaction analysis using QCM-D proved that hemicelluloses moderate the interaction between CNFs and CNFs prepared from softwood pulp (SW-CNFs) containing galactoglucomannan is stronger than CNFs prepared from hardwood pulp (HW-CNFs) containing mainly glucuronoxylan. It was suggested that hemicellulose contributes to improved dispersion stability and increased viscosity in the aqueous state irrespective of the type of hemicellulose. However, the strength of the interaction between CNFs, which is dependent on the type of hemicellulose, did not relate directly with the dispersion stability and the viscosity characteristic. The physical properties of CNFs prepared from kraft pulps in the aqueous state are determined by several factors, such as the morphologies of the CNFs and the physical properties of hemicellulose.

Funding This research received no specific grant from any funding agency in the public, commercial, or not-for-profit sectors.

Availability of data and material The data during and/or analyzed during the current study available from the corresponding author on reasonable request.

Compliance with ethical standards

Conflicts of interest The authors declare that they have no conflict of interest.

References

Ahola S, Salmi J, Johansson LS, Laine J, Österberg M (2008) Model films from native cellulose nanofibrils. Preparation, swelling, and surface interactions. Biomacromol 9:1273–1283

Arola S, Malho JM, Laaksonen P, Lillea M, Linde MB (2013) The role of hemicellulose in nanofibrillated cellulose networks. Soft Matter 9:1319–1326

Eronen P, Österberg M, Heikkinen S, Tenkanen M, Laine J (2011) Interactions of structurally different hemicelluloses with nanofibrillar cellulose. Carbohyd Polym 86:1281–1290

Grüneberger F, Künniger T, Zimmermann T, Arnold M (2014) Rheology of nanofibrillated cellulose/acrylate systems for coating applications. Cellulose 21:1313–1326

Höök F, Rodahl M, Brzezinski P, Kasemo B (1998) Energy dissipation kinetics for protein and antibody-antigen adsorption under shear oscillation on a quartz crystal microbalance. Langmuir 14:729–734

Isogai A, Saito T, Fukuzumi H (2011) TEMPO-oxidized cellulose nanofibers. Nanoscale 3:71–85

Iwamoto S, Endo T (2015) 3 nm thick lignocellulose nanofibers obtained from esterified wood with maleic anhydride. ACS Macro Lett 4:80–83

Iwamoto S, Abe K, Yano H (2008) The effect of hemicelluloses on wood pulp nanofibrillation and nanofiber network characteristics. Biomacromol 9:1022–1026

Iwamoto S, Lee SH, Endo T (2014) Relationship between aspect ratio and suspension viscosity of wood cellulose nanofibers. Polym J 46:73–76

Klemm D, Kramer F, Moritz S, Lindström T, Ankerfors M, Gray D, Dorris A (2011) Nanocelluloses: a new family of nature-based materials. Angew Chem Int Ed 50:5438–5466

Kulasinski K, Guyer R, Derome D, Carmelie J (2015) Water adsorption in wood microfibril-hemicellulose system: role of the crystalline–amorphous interface. Biomacromol 16:2972–2978

Kumagai A, Endo T (2018) Comparison of the surface constitutions of hemicelluloses on lignocellulosic nanofibers prepared from softwood and hardwood. Cellulose 25:3885–3897

Kumagai A, Lee SH, Endo T (2013) Thin film of lignocellulosic nanofibrils with different chemical composition for QCM-D study. Biomacromol 14:2420–2426

Kumagai A, Endo T, Adachi M (2019) Evaluation of cellulose nanofibers by using sedimentation method. Jpn Tappi J 73:461–469

Lasseuguette E, Roux D, Nishiyama Y (2008) Rheological properties of microfibrillar suspension of TEMPO-oxidized pulp. Cellulose 15:425–433

Li MC, Wu Q, Song K, Lee S, Qing Y, Wu Y (2015) Cellulose nanoparticles: structure–morphology–rheology relationships. ACS Sustainable Chem Eng 3:821–832

Mendoza L, Gunawardhana T, Batchelor W, Garnier G (2018) Effects of fibre dimension and charge density on nanocellulose gels. J Colloid Interface Sci 525:119–125

Nechyporchuk O, Belgacem MN, Pignon F (2016) Current progress in rheology of cellulose nanofibril suspensions. Biomacromol 17:2311–2320

Noguchi Y, Homma I, Matsubara Y (2017) Complete nanofibrillation of cellulose prepared by phosphorylation. Cellulose 24:1295–1305

Olejnik A, Schoreder G, Nowak I (2015) The tetrapeptide N-acetyl-Pro-Pro-Tyr-Leu in skin care formulations—physicochemical and release studies. Int J Pharm 492:161–168

Pääkkö M, Ankerfors M, Kosonen H, Nykänen A, Ahola S, Österberg M, Ruokolainen J, Laine J, Larsson PT, Ikkala O, Lindström T (2007) Enzymatic hydrolysis combined with mechanical shearing and high-pressure homogenization for nanoscale cellulose fibrils and strong gels. Biomacromol 8:1934–1941

Pennells J, Godwin ID, Amiralian N, Martin DJ (2020) Trends in the production of cellulose nanofibers from non-wood sources. Cellulose 27:575–593

Penttilä PA, Várnai A, Pere J, Tammelin T, Salmén L, Siika-aho M, Viikari L, Serimaa R (2013) Xylan as limiting factor in enzymatic hydrolysis of nanocellulose. Bioresour Technol 129:135–141

Reviakine I, Johannsmann D, Richter RP (2011) Hearing what you cannot see and visualizing what you hear: interpreting quartz crystal microbalance data from solvated interfaces. Anal Chem 83:8838–8848

Rodahl M, Höök F, Krozer A, Brzezinski P, Kasemo B (1995) Quartz crystal microbalance setup for frequency and Q-factor measurements in gaseous and liquid environments. Rev Sci Instrum 66:3924–3930

Salmén L, Olsson AM (1998) Interaction between hemicelluloses, lignin and cellulose: structure-property relationships. J Pulp Pap Sci 24:99–103

Sauerbrey G (1959) The use of quartz oscillators for weighing thin layers and for microweighing. Z Phys 155:206–222

Scheller HV, Ulvskov P (2010) Hemicelluloses. Annu Rev Plant Biol 61:263–289

Siró I, Plackett D (2010) Microfibrillated cellulose and new nanocomposite materials: a review. Cellulose 17:459–494

Solala I, Iglesias MC, Peresin MS (2020) On the potential of lignin-containing cellulose nanofibrils (LCNFs): a review on properties and applications. Cellulose 27:1853–1877

Stelte W, Sanadi AR (2009) Preparation and characterization of cellulose nanofibers from two commercial hardwood and softwood pulps. Ind Eng Chem Res 48:11211–11219

Tammelin T, Saarinen T, Österberg M, Laine J (2006) Preparation of Langmuir/Blodgett-cellulose surfaces by using horizontal dipping procedure. Application for polyelectrolyte adsorption studies performed with QCM-D. Cellulose 13:519–535

Tammelin T, Paananen A, Österberg M (2009) Hemicelluloses at interfaces: some aspects of the interactions. In: Lucian LA, Rojas OJ (eds) The nanoscience and technology of renewable biomaterials. Wiley, Chichester, pp 149–172

Tenhunen TM, Peresin MS, Penttilä PA, Pere J, Serimaa R, Tammelin T (2014) Significance of xylan on the stability and water interactions of cellulosic nanofibrils. React Func Polym 85:157–166

Tokoh C, Takabe K, Sugiyama J, Fujita M (2002) Cellulose synthesized by Acetobacter xylinum in the presence of plant cell wall polysaccharides. Cellulose 9:65–74

Voinova M, Rodahl M, Jonson M, Kasemo B (1999) Viscoelastic acoustic response of layered polymer films at fluid-solid interfaces: continuum mechanics approach. Phys Scr 59:391–396

Yadong Z, Moser C, Lindström ME, Henriksson G, Li J (2017) Cellulose nanofibers from softwood, hardwood, and tunicate: preparation–structure–film performance interrelation. ACS Appl Mater Interfaces 9:13508–13519